applied sciences

MDPI

Article

Synthesis, Tyrosinase Inhibiting Activity and Molecular Docking of Fluorinated Pyrazole Aldehydes as Phosphodiesterase Inhibitors

Vesna Rastija [1], Harshad Brahmbhatt [2], Maja Molnar [2], Melita Lončarić [2], Ivica Strelec [2], Mario Komar [2] and Valentina Pavić [3,*]

1 Faculty of Agrobiotechnical Sciences Osijek, Josip Juraj Strossmayer University of Osijek, Vladimira Preloga 1, 31000 Osijek, Croatia; vrastija@fazos.hr
2 Faculty of Food Technology Osijek, Josip Juraj Strossmayer University of Osijek, Franje Kuhača 20, 31000 Osijek, Croatia; brahmbhattharshad@hotmail.com (H.B.); maja.molnar@ptfos.hr (M.M.); melita.loncaric@ptfos.hr (M.L.); ivica.strelec@ptfos.hr (I.S.); mario.komar@ptfos.hr (M.K.)
3 Department of Biology, Josip Juraj Strossmayer University of Osijek, Cara Hadrijana 8/A, 31000 Osijek, Croatia
* Correspondence: vpavic@biologija.unios.hr; Tel.: +385-31-399-933

Received: 6 March 2019; Accepted: 19 April 2019; Published: 25 April 2019

Abstract: A series of fluorinated 4,5-dihydro-1*H*-pyrazole derivatives were synthesized in the reaction of corresponding acetophenone and different aldehydes followed by the second step synthesis of desired compounds from synthesized chalcone, hydrazine hydrate, and formic acid. Structures of all compounds were confirmed by both ^{1}H and ^{13}C NMR and mass spectrometry. Antibacterial properties of compounds were tested on four bacterial strains, *Escherichia coli*, *Pseudomonas aeruginosa*, *Bacillus subtilis*, and *Staphylococcus aureus*. Among synthesized compounds, the strongest inhibitor of monophenolase activity of mushroom tyrosinase (32.07 ± 3.39%) was found to be *5-(2-chlorophenyl)-3-(4-fluorophenyl)-4,5-dihydro-1H-pyrazole-1-carbaldehyde*. The PASS program has predicted the highest probable activity for the phosphodiesterase inhibition. To shed light on molecular interactions between the synthesized compounds and phosphodiesterase, all compounds were docked into the active binding site. The obtained results showed that the compound with the dimethoxyphenyl ring could be potent as an inhibitor of phosphodiesterase, which interacts in PDE5 catalytic domain of the enzyme. Key interactions are bidentate hydrogen bond (H-bond) with the side-chain of Gln817 and van der Waals interactions of the dimethoxyphenyl ring and pyrazole ring with hydrophobic clamp, which contains residuals, Val782, Phe820, and Tyr612. Interactions are similar to the binding mode of the inhibitor sildenafil, the first oral medicine for the treatment of male erectile dysfunction.

Keywords: fluorinated pyrazole aldehydes; tyrosinase inhibition; phosphodiesterase inhibition; antibacterial activity; molecular docking

1. Introduction

Pyrazoles are nitrogen-containing aromatic heterocycles possessing a five-membered ring in their structure, with two nitrogen atoms in an adjacent position [1]. Catalytic hydrogenation of pyrazoles yields 4,5-dihydro-1*H*-pyrazoles or 2-pyrazoline (Figure 1) [2].

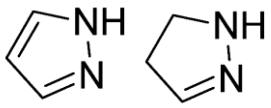

Figure 1. Structure of pyrazole and 4,5-dihydro-1*H*-pyrazole.

4,5-Dihydro-1*H*-pyrazoles are often synthesized in cyclocondensation of chalcones with hydrazine hydrate, while chalcones are formed in the reaction between aldehydes and acetophenones in the presence of NaOH [3], KOH [4,5]. Zhou et al. [6] synthesized chalcones in the presence of neutral Al_2O_3 and KOH under microwave irradiation, which in reaction with the hydrazine hydrate yielded *N*-4,5-dihydro-1*H*-pyrazoles with tyrosinase inhibiting activity.

In general, pyrazoline derivatives exhibit a variety of biological activities, depending on the substituents, which can be placed at a different position of the ring [2]. The accumulation of the fluorine on the carbon atom causes increased oxidative and thermal stability of the drugs as well as increased lipid solubility, which accelerates the drug absorption and transport in vivo [7]. Introduction of fluorine to the drug molecules can reduce their in vivo metabolic turnover by blocking potential reactive positions with fluorine and improving the stability of the molecule toward acid hydrolysis [8]. The biological activity of pyrazoline derivatives includes anticancer activity, especially fluorinated derivatives [9], anti-inflammatory activity [10,11], and anticonvulsant activity [12]. Antifertility, antibacterial, and antifungal agents are frequently fluorinated pyrazolines and pyrazoles [13]. They have also been investigated in inhibitory nNOS activity in rat brains and proven very effective [14]. Fused 4,5-dihydro-1*H*-pyrazoles were found to be an excellent antibacterial agent against *Staphylococcus aureus* and *Corynebacterium diphtheriae* [15], while 5-aryl-1-carboxamidino-3-styryl-4,5-dihydro-1*H*-pyrazoles were found to be potent antioxidants and antimicrobial agents against *Salmonella typhi, Staphylococcus aureus,* and *Streptococcus pneumoniae* [16]. An excellent antibacterial activity of 4,5-dihydro-1*H*-pyrazole derivatives was also proven against *Pseudomonas aeruginosa, Escherichia coli*, *Bacillus subtilis,* and *Staphylococcus aureus*, showing a potent DNA gyrase inhibitory activity as well [17]. All the described above indicates that 4,5-dihydro-1*H*-pyrazoles are very potent bioactive compounds and their structural modifications, especially the introduction of a fluorine atom on a phenyl ring, could lead to their increased bioactivity.

The growing necessity for new and potent antibiotics, due to the microorganism resistance to the existing antibiotics, has led us to synthesize pyrazole derivatives as potential antimicrobials. Thus, the aim of this work was to synthesize fluorinated 4,5-dihydro-1*H*-pyrazole derivatives in order to examine their antibacterial activity. Since 4,5-dihydro-1*H*-pyrazoles have already proven to inhibit tyrosinase activity [6], and this enzyme is responsible for human hyperpigmentation as well as browning reactions, we also investigated the compound's tyrosinase inhibiting activity. In order to indicate the other biological activity of synthesized compounds, in silico prediction according to the structural formulas was performed, as well as molecular docking to evaluated interactions of the ligand with the compatible enzyme.

2. Materials and Methods

2.1. General

All chemicals used within this research were acquired from commercial suppliers. Aluminum TLC plates coated with fluorescent indicator F254 were used for thin-layer chromatography, with benzene:acetic acid:acetone (8:1:1) as an eluent, and checked under a UV lamp (HP-UVIS® UV-analysis lamp, Biostep GmbH –Desaga, Burkhardtsdorf, Germany) on 365 nm and 254 nm. NMR spectra were recorded on Bruker Avance 600 MHz NMR Spectrometer (Bruker Biospin GmbH, Rheinstetten, Germany) at 293 K with DMSO-d_6 used as a solvent and tetramethylsilane (TMS) as an internal standard. The mass spectra were recorded by LC/MS/MS API 2000 (Applied Biosystems /MDS SCIEX, Redwood City, CA, USA). Melting points were determined with electrothermal melting point

apparatus (Electrothermal Engineering Ltd., Rochford, UK). Bacteria strains were isolates from various clinical specimens obtained from Microbiology Service of the Public Health Institute of Osijek-Baranja County, Osijek, Croatia.

*2.2. General Procedure for Synthesis of Fluorinated Pyrazoles (**3a**–**j**)*

All compounds were synthesized according to Rostom et al. [18]. Briefly, equimolar amounts of desired acetophenone and aldehyde were mixed together in cold methanol and 50% aqueous NaOH solution was added. The mixture was stirred for 4 h and poured over crushed ice, the product was filtered and dried.

The second step included synthesis of desired compounds from synthesized chalcone, hydrazine hydrate and formic acid under reflux for 10 h. The mixture was cooled, the obtained precipitate filtered and dried.

*3-(4-fluorophenyl)-5-(4-methoxyphenyl)-4,5-dihydro-1H-pyrazole-1-carbaldehyde (**3a**)*

Mp = 131–132 °C; Rf = 0.81; ^{1}H NMR (300 MHz, ppm, DMSO-d_6): 8.87 (s, 1H, −CHO); 7.86–7.84 (m, 2H, arom.), 7.33–7.32 (m, 2H, arom.), 7.17–7.15 (d, 2H, arom.), 6.90–6.89 (d, 2H, arom.), 5.50–5.47 (m, 1H, CH-pyr.), 3.91–3.86 (m, 1H, −CH_2-pyr.), 3.73 (s, 3H, OCH_3), 3.22–3.18 (m, 1H, CH_2-pyr.); ^{13}C NMR (DMSO-d_6) δ (ppm): 164.1, 162.5, 159.5, 158.6, 155.2, 133.3, 129.2, 129.1, 127.0, 115.9, 115.8, 114.0, 58.1, 55.1, 42.3; MS: *m/z* calcd for $[C_{17}H_{15}FN_2O_2]$+ ([M+H]+/M++H+Na): 298.31, found 299.0/321.20.

*3-(4-fluorophenyl)-5-(2-methoxyphenyl)-4,5-dihydro-1H-pyrazole-1-carbaldehyde (**3b**)*

Mp = 110–112 °C; Rf = 0.84; ^{1}H NMR (300 MHz, ppm, DMSO-d_6): 8.91 (s, 1H, −CHO); 7.85–7.80 (m, 2H, arom.), 7.32–7.25 (m, 3H, arom.), 7.06–6.99 (d, 2H, arom.), 6.92–6.87 (d, 1H, arom.), 5.67–5.61 (m, 1H, CH-pyr.), 3.91–3.86 (m, 1H, −CH_2-pyr.), 3.80 (s, 3H, OCH_3), 3.09–3.02 (m, 1H, CH_2-pyr.); ^{13}C NMR (DMSO-d_6) δ (ppm): 165.4, 162.1, 160.0, 156.4, 156.1, 129.6 (d, J = 8.78 Hz), 129.3, 128.7, 127.9, 126.4, 120.8, 116.5, 116.2, 111.9, 56.3, 55.1, 41.8; *m/z* calcd for $[C_{17}H_{15}FN_2O_2]$+ ([M+H]+/M++H+Na): 298.31, found 299.20/321.10.

*5-(3-fluorophenyl)-3-(4-fluorophenyl)-4,5-dihydro-1H-pyrazole-1-carbaldehyde (**3c**)*

Mp = 157 °C; Rf = 0.85; ^{1}H NMR (300 MHz, ppm, DMSO-d_6): 8.91 (s, 1H, −CHO); 7.86–7.84 (m, 2H, arom.), 7.42–7.39 (m, 1H, arom.), 7.33–7.31 (m, 2H, arom.), 7.13–7.08 (d, 3H, arom.), 5.58–5.56 (m, 1H, CH-pyr.), 3.95–3.90 (m, 1H, −CH_2-pyr.), 3.28–3.24 (m, 1H, CH_2-pyr.); ^{13}C NMR (DMSO-d_6) δ (ppm): 164.2, 163.1, 162.5, 161.5, 159.7, 155.2, 143.9, 130.8 (d, J = 8.41 Hz), 129.1 (d, J = 8.41 Hz), 127.3, 121.7 (d, J = 2.40 Hz), 115.9, 114.4, 114.2, 112.8, 112.7, 58.1, 42.2; MS: *m/z* calcd for $[C_{16}H_{12}F_2N_2O]$+ ([M+H]+/M++H+Na): 286.28, found 287.10/309.20.

*(E)-3-(4-fluorophenyl)-5-(4-styrylphenyl)-4,5-dihydro-1H-pyrazole-1-carbaldehyde (**3d**)*

Mp = 157 °C; Rf = 0.86; ^{1}H NMR (300 MHz, ppm, DMSO-d_6): 8.86 (s, 1H, −CHO); 7.85–7.80 (m, 2H, arom.), 7.44–7.42 (m, 2H, arom.), 7.34–7.28 (m, 5H, arom.), 6.60–6.56 (d, 1H, styryl), 6.36–6.28 (q, 1H, styryl), 5.20–5.12 (m, 1H, CH-pyr.), 3.73–3.64 (m, 1H, −CH_2−pyr.), 3.29–3.22 (m, 1H, CH_2-pyr.); ^{13}C NMR (DMSO-d_6) δ (ppm): 165.4, 162.2, 160.3, 156.1, 136.2, 135.4, 134.4, 134.1, 132.9, 131.3, 129.9, 129.6, 129.4, 129.1, 128.3, 128.1, 127.7, 127.2, 126.9, 116.5, 116.2, 57.7; *m/z* calcd for $[C_{24}H_{19}FN_2O]$+ ([M+H]+/M++H+Na): 370.42, found 371.3/393.20.

*3-(4-fluorophenyl)-5-(3-methoxyphenyl)-4,5-dihydro-1H-pyrazole-1-carbaldehyde (**3e**)*

Mp = 143–145 °C; Rf = 0.83; ^{1}H NMR (300 MHz, ppm, DMSO-d_6): 8.91 (s, 1H, −CHO); 7.86–7.83 (m, 2H, arom.), 7.33–7.25 (m, 3H, arom.), 7.33–7.31 (m, 2H, arom.), 6.86–6.84 (m, 1H, arom.), 6.80–6.78 (m, 2H, arom.), 5.53–5.50 (m, 1H, CH-pyr.), 3.93–3.88 (m, 1H, −CH_2-pyr.), 3.74 (s, 3H, OCH_3), 3.23–3.19 (m, 1H, CH_2-pyr.); ^{13}C NMR (DMSO-d_6) δ (ppm): 164.2, 162.5, 159.6, 159.5, 155.2, 142.8, 129.9, 129.1 (d, J = 2.40 Hz), 127.3, 117.5, 115.9, 115.8, 112.7, 111.6, 58.5, 52.0, 42.4; *m/z* calcd for $[C_{17}H_{15}FN_2O_2]$+ ([M+H]+/M++H+Na): 298.31, found 299.0/321.20.

*3-(4-fluorophenyl)-5-(2-hydroxyphenyl)-4,5-dihydro-1H-pyrazole-1-carbaldehyde (***3f***)*

Mp = 204–206 °C; Rf = 0.74; ^{1}H NMR (300 MHz, ppm, DMSO-d_6): 9.74 (s, 1H, OH), 8.91 (s, 1H, −CHO); 7.85–7.80 (m, 2H, arom.), 7.32–7.26 (m, 2H, arom.), 7.33–7.31 (m, 2H, arom.), 7.12–7.07 (t, 1H, arom.), 6.95–6.92 (d, 1H, arom.), 6.86–6.83 (d, 1H, arom.), 6.76–6.71 (t, 1H, arom.), 5.64–5.58 (m, 1H, CH-pyr.), 3.90–3.80 (m, 1H, −CH_2-pyr.), 3.12–3.05 (m, 1H, CH_2-pyr.); ^{13}C NMR (DMSO-d_6) δ (ppm): 165.4, 162.1, 160.0, 156.1, 154.6, 129.5 (d, *J* = 8.78 Hz), 128.9, 128.1, 128.0, 127.0, 126.8, 119.3, 116.5, 116.2, 115.9, 53.4; *m/z* calcd for $[C_{16}H_{13}FN_2O_2]$+ (M++H+Na): 284.29, found 307.22.

*5-(2,5-dimethoxyphenyl)-3-(4-fluorophenyl)-4,5-dihydro-1H-pyrazole-1-carbaldehyde (***3g***)*

Mp = 153 °C; Rf = 0.82; ^{1}H NMR (300 MHz, ppm, DMSO-d_6): 8.91 (s, 1H, −CHO); 7.84–7.82 (m, 2H, arom.), 7.31–7.28 (m, 2H, arom.), 6.99–6.97 (d, 1H, arom.), 6.85–6.83 (d, 1H, arom.), 6.56–6.55 (d, 1H, arom.), 5.61–5.58 (m, 1H, CH-pyr.), 3.88–3.83 (m, 1H, −CH_2-pyr.), 3.75 (s, 3H, OCH_3), 3.66 (s, 3H, OCH_3), 3.08–3.05 (m, 1H, CH_2-pyr.); ^{13}C NMR (DMSO-d_6) δ (ppm): 164.1, 162.5, 159.6, 155.6, 153.1, 150.0, 130.0, 129.4, 129.0 (d, *J* = 9.61 Hz), 127.5, 115.9, 115.8, 112.7, 112.5 (d, *J* = 13.22 Hz), 56.0, 55.3, 54.6, 41.3; *m/z* calcd for $[C_{18}H_{17}FN_2O_3]$+ (M++H+Na): 328.34, found 351.20.

*5-(4-bromophenyl)-3-(4-fluorophenyl)-4,5-dihydro-1H-pyrazole-1-carbaldehyde (***3h***)*

Mp = 144 °C; Rf = 0.85; ^{1}H NMR (300 MHz, ppm, DMSO-d_6): 8.89 (s, 1H, −CHO); 7.85–7.83 (m, 2H, arom.), 7.55–7.53 (d, 2H, arom.), 7.33–7.30 (m, 2H, arom.), 7.22–7.20 (d, 2H, arom.), 5.55–5.52 (m, 1H, CH-pyr.), 3.94–3.89 (m, 1H, −CH_2-pyr.), 3.25–3.21 (m, 1H, CH_2-pyr.); ^{13}C NMR (DMSO-d_6) δ (ppm): 164.2, 162.5, 159.7, 155.2, 140.6, 131.6, 129.2, 129.1, 128.1, 127.3, 120.5, 115.9, 115.8, 58.1, 42.1; *m/z* calcd for $[C_{16}H_{12}BrFN_2O]$+ (M++H+Na): 347.18, found 369.00.

*5-(2-chlorophenyl)-3-(4-fluorophenyl)-4,5-dihydro-1H-pyrazole-1-carbaldehyde (***3i***)*

Mp = 125–127 °C; Rf = 0.86; ^{1}H NMR (300 MHz, ppm, DMSO-d_6): 8.96 (s, 1H, −CHO); 7.87–7.82 (m, 2H, arom.), 7.53–7.50 (m, 1H, arom.), 7.34–7.28 (m, 4H, arom.), 7.17–7.14 (m, 1H, arom.), 5.79–5.73 (m, 1H, CH-pyr.), 4.06–3.96 (m, 1H, −CH_2-pyr.), 3.19–3.12 (m, 1H, CH_2-pyr.); ^{13}C NMR (DMSO-d_6) δ (ppm): 165.5, 162,2, 160,1, 155.8, 138.3, 131.4, 130.2, 129.7, 129.6, 129.5, 128.2, 127.2, 116.5, 116.2, 56.9, 41.8; *m/z* calcd for $[C_{16}H_{12}ClFN_2O]$+ ([M+H]+/M++H+Na): 302.73, found 303.20/325.10.

*5-(4-(dimethylamino)phenyl)-3-(4-fluorophenyl)-4,5-dihydro-1H-pyrazole-1-carbaldehyde (***3j***)*

Mp = 168–171 °C; Rf = 0.13; ^{1}H NMR (300 MHz, ppm, DMSO-d_6): 8.86 (s, 1H, −CHO); 7.86–7.83 (m, 2H, arom.), 7.33–7.30 (m, 2H, arom.), 7.05–7.04 (d, 2H, arom.), 6.68–6.66 (d, 2H, arom.), 5.43–5.40 (m, 1H, CH-pyr.), 3.87–3.82 (m, 1H, −CH_2-pyr.), 3.19–3.16 (m, 1H, CH_2-pyr.), 2.86 (s, 6H, $2CH_3$); ^{13}C NMR (DMSO-d_6) δ (ppm): 164.2, 162.5, 159.4, 155.1, 149.9, 129.0, 128.9, 128.7, 127.5, 126.5, 115.9, 115.8, 112.4, 58.3, 42.2, 40.1; *m/z* calcd for $[C_{18}H_{18}FN_3O]$+ ([M+H]+/M++H+Na): 311.35, found 312.30/334.

2.3. Antibacterial Susceptibility Testing

Antibacterial properties against *Bacillus subtilis* and *Staphylococcus aureus* as two Gram-positive, and *Escherichia coli* and *Pseudomonas aeruginosa* as Gram-negative bacterial strains were tested for all synthesized compounds. Working cultures were grown overnight in Mueller-Hinton broth (MHB) (Fluka, BioChemica, Germany) under optimal conditions (37 °C with 50% humidity). Modified broth microdilution method [17] was used for MIC values determination as described in our previous work [18]. One hundred microliters of bacterial cultures in MHB was added to 100 µL of a serially diluted compound (250 to 0.122 µg mL^{-1}) in sterile TPP 96-well plates (TPP Techno Plastic Products AG Trasadingen, Switzerland). Growth control and background control were included in each plate in amounts corresponding to the highest amount in the test solution and subtracted from the results. The antibacterial standard amikacin sulphate was co-assayed under the same conditions in concentration range of 0.122–250 µg mL^{-1}. After incubation at 37 °C for 24 h in an atmospheric incubator with 5% CO_2 and 50% humidity, an additional incubation for three hours at 37 °C was

performed with triphenyl tetrazolium chloride as a reducing agent indicator for microbial growth. The lowest concentrations of compound at which there was no color change or visual turbidity due to microbial growth was defined as the MIC value, derived from triplicate analyses and expressed as micrograms per milliliter.

2.4. Tyrosinase Inhibiting Activity

All synthesized compounds were tested for monophenolase and diphenolase inhibitory activity of mushroom tyrosinase according to a slightly modified procedure of Molnar et al. [19]. In brief, reaction mixture (1 mL) for determination of monophenolase activity contained 100 U of mushroom tyrosinase, 1 mM L-tyrosine and 100 µM inhibitor, while for diphenolase activity 0.5 mM L-DOPA instead L-tyrosine. In both cases, final phosphate buffer (pH 6.5) concentration in the reaction mixture was 100 mM, and the amount of DMSO was 1%.

IC50 value was determined for kojic acid by nonlinear regression using a dose-response inhibition model using GraphPad Prism version 7.00 for Windows (GraphPad Software, La Jolla, CA, USA).

2.5. Docking Studies

Selection of the biological activity for docking study was done with the help of computer program PASS [20]. Software estimates predicted activity spectrum of a compound according to the structural formulas of synthesized fluorinated pyrazole aldehydes as probable activity (Pa) and probable inactivity (Pi). Activity with Pa > Pi is considered as possible for a particular compound. Phosphodiesterase inhibition has been selected for docking study since the PASS program calculated Pa > Pi of all compounds for that activity.

The molecular docking of compounds (**3a–j**) was performed using iGEMDOCK (BioXGEM, Taiwan). Crystal coordinates of the catalytic domain of phosphodiesterase type 5 (PDE5) (PDB ID: 4OEW) in the complex with monocyclic pyrimidinones (PDB ID: 5IO) were downloaded from Protein Data Bank (PDB, https://www.rcsb.org/). The PDE5 structure was prepared, including the removal of water molecules and optimized protein structure using BIOVIA Discovery Studio 4.5 (Dassault Systèmes, San Diego, CA, USA). Avogadro 1.2.0 (University of Pittsburgh, Pittsburgh, PA, USA) was applied for optimizing the 3D structures of 28 molecules using the molecular mechanic's force field (MM+) [21]. In addition, the semiempirical PM3 method was used for geometry optimization of all structures [22].

The protein binding site was outlined according to the bounded ligand (PDB ID: 5IO) [23]. Genetic parameters were set (population size 200, generations 70, the number of a solution or poses: 2) after the preparation of the protein target and set of optimized structures of 10 fluorinated pyrazoles as ligands. Docking into the binding site and generation of protein-compound interaction profiles of electrostatic (*Elec*), hydrogen-bonding (*Hbond*), and van der Waals (*vdW*) interactions was performed for each compound in the library. Finally, by combining pharmacological interactions and energy-based scoring function, the compounds were ranked. Energy-based scoring function or total energy (*E*) is:

$$E = vdW + Hbond + Elec. \quad (1)$$

3. Results and Discussion

Desired 4,5-dihydro-1*H*-pyrazole derivatives were synthesized from corresponding chalcones. Chalcones were obtained in the typical aldol condensation reaction of aldehydes and acetophenones, while pyrazoles were synthesized from corresponding chalcones in the presence of hydrazine hydrate and formic acid (Figure 2). Their structures were confirmed by ^{1}H NMR, ^{13}C NMR, and mass spectra. All compounds show characteristic peaks for –CHO proton around 8.67 ppm, pyrazole C-5 proton peak around 5.58 ppm and pyrazole C-4 proton peaks around 3.24 ppm and 3.90 ppm. Other peaks correspond to aromatic protons (6.90–7.90 ppm) and specific substituents on the phenyl

ring. Mass spectra for each compound corresponds to its molar mass. All compounds were further characterized by their melting points and R_f values as indicated in the Materials and Methods Section.

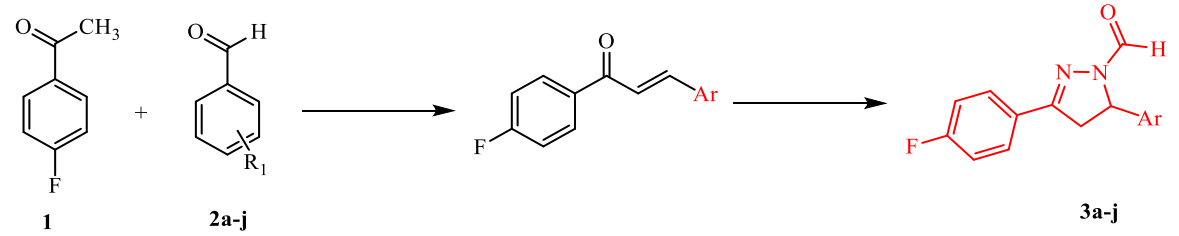

a - p-OCH_3-phenyl
b - 2-OCH_3-phenyl
c - 3-fluorophenyl
d - 4-styrylphenyl
e - 3-OCH_3-phenyl
f - 2-OH-phenyl
g - 2,5-$(OCH_3)_2$-phenyl
h - 4-bromophenyl
i - 2-chlorophenyl
j - 4-dimethylaminophenyl

Figure 2. Synthetic pathway for fluorinated pyrazole aldehydes.

After synthesis, purification, and full characterization, all compounds were investigated for their antibacterial activity against two Gram-positive and two Gram-negative bacteria (Table 1) and tyrosinase inhibiting activity (Table 2).

Table 1. Antibacterial activity of synthesized compounds in terms of minimum inhibitory concentration (MIC) against *Escherichia coli*, *Pseudomonas aeruginosa*, *Bacillus subtilis* and *Staphylococcus aureus* (μg mL^{-1}).

Compound	Minimum Inhibitory Concentration (μg mL^{-1})			
	E. coli	*P. aeruginosa*	*B. subtilis*	*S. aureus*
3a	62.5	62.5	62.5	62.5
3b	62.5	62.5	62.5	62.5
3c	62.5	62.5	62.5	62.5
3d	62.5	62.5	62.5	62.5
3e	62.5	62.5	62.5	62.5
3f	62.5	62.5	62.5	62.5
3g	62.5	62.5	125	125
3h	62.5	62.5	250	250
3i	62.5	62.5	250	250
3j	62.5	62.5	250	250
amikacin	1.95	0.49	0.24	1.95

Table 2. Tyrosinase inhibiting activity of synthesized compounds *.

Compound	Monophenolase Inhibition Rate (%)	Diphenolase Inhibition Rate (%)
3a	10.84 ± 1.20	21.08 ± 1.86
3b	5.22 ± 1.84	15.98 ± 3.25
3c	0.21 ± 1.39	10.11 ± 3.92
3d	28.80 ± 4.10	22.81 ± 0.33
3e	21.74 ± 2.82	16.55 ± 0.29
3f	20.11 ± 1.63	13.67 ± 0.50
3g	25.54 ± 2.49	14.34 ± 0.88
3h	24.46 ± 3.77	20.79 ± 0.17
3i	32.07 ± 3.39	15.11 ± 0.50
3j	25.54 ± 4.10	18.38 ± 1.01
Kojic acid	100 ± 0.00	88.45 ± 0.83

* concentration of tested compound in the reaction mixture was 100 μM. Results present mean value ± standard deviation of triplicate measurements.

The antibacterial assay revealed that Gram-negative bacteria were more susceptible to the tested compounds than Gram-positive ones. The cell wall of Gram-positive bacteria ranges from 20 to 80 nm, while for Gram-negative bacteria it ranges from 1.5 to 10 nm [24,25]. Of the four tested bacteria, the Gram-positive had higher resistance against tested compounds, with up to threefold higher MIC values (62.5–250 μg mL^{-1} for *B. subtilis* and *S. aureus*) than for Gram-negative bacteria (62.5 μg mL^{-1} for *E. coli* and *P. aeruginosa* for all tested compounds). Electrostatic interactions can regulate the interaction of the bacterial surface with acidic and basic functional groups and various agents, which can lead to changed cell surface permeability and thus lead to the death of the cell. The target protein often tolerates the replacement of a hydrogen atom with fluorine, since it has a small atom volume. In order to increase the half-life of the drug and human exposure, many drugs on the market contain introduced fluorine atoms [26]. The introduction of a fluorine atom into a molecule can change the distribution of electrons and thus affect pKa, dipole moment, and even chemical reactivity and stability of adjacent functional groups since it is the most electronegative element. The bioavailability of the compounds can also be improved by higher membrane permeability for the compound as a result of reduced compound basicity due to the introduced fluorine [27]. Threefold higher MIC was found with the compounds **3h–j** that had various halogen (bromo/chloro) or dimethylamino group containing substituents implying that electrostatic distribution affects membrane permeation of the compound.

Determination of tyrosinase inhibitory potential revealed that none of the compounds significantly inhibited mushroom tyrosinase at 100 μM concentration, in comparison with the kojic acid as a standard inhibitor, which exhibited IC_{50} of 16.96 ± 1.05 μM for monophenolase, and 13.10 ± 1.02 μM for diphenolase activity. Nevertheless, in most cases, greater tyrosinase inhibition could be observed for monophenolase than diphenolase activity. Among synthesized compounds, compound **3i** was found as the strongest inhibitor of monophenolase activity of mushroom tyrosinase (32.07 ± 3.39%), but its inhibiting activity of diphenolase activity was found twofold lower. The most probable reason for the lack of significant tyrosinase inhibitory activity of synthesized compounds is pyrazole ring *N*-substitution with aldehyde group. Zhou et al. (2013) have described that *N*-acetylation at pyrazole ring causes diminished inhibitory activity when compared to non-substituted compounds [6]. In addition, based on the report of Zhou et al. [6] it seems obvious that presence of hydroxyl groups on phenyl rings might be the prerequisite for tyrosinase inhibiting activity, which was not the case in the present study where phenyl ring A was fluorinated, and ring B had a various non-hydroxyl group containing substituents.

Experimentally proven inactivity of synthesized compounds towards mushroom tyrosinase was the motive to find another potential biological activity for these compounds. PASS online program (http://www.pharmaexpert.ru/passonline/) provides the prediction of several hundred biological activities based on structural formulas. For almost all synthesized compounds PASS program has predicted the highest *Pa* for the phosphodiesterase inhibition. All the compounds showed greater *Pa* than *Pi* (Table 3).

Table 3. Results of PASS program for the phosphodiesterase inhibition.

Compound	*Pa* *	*Pi*
3a	0.651	0.004
3b	0.584	0.004
3c	0.616	0.004
3d	0.516	0.004
3e	0.637	0.004
3f	0.396	0.005
3g	0.611	0.004
3h	0.469	0.004
3i	0.508	0.004
3j	0.460	0.005

* probable activity (*Pa*) and probable inactivity (*Pi*).

Phosphodiesterase type 5 (PDE5) is a cyclic guanosine monophosphate (cGMP-specific) enzyme and mostly expressed in smooth muscle tissue of corpus cavernosum. PDE5 inhibitors have vasodilative effects, therefore, are used for treating erectile dysfunction, pulmonary hypertension and cardiovascular diseases [28]. In order to provide virtual screening of synthesized compounds as potential inhibitors of PDE5 molecular docking study was performed. Docking score and energy of interactions between protein residue and ligand are tabulated in Table 4.

Table 4. Docking scores for fluorinated pyrazoles in interaction with PDE5.

Comp.	Pose	Total Energy/kcal mol^{-1}	Van Der Waals Interaction	*H Bond*	*Elec*
3g	1	−105.62	−95.34	−10.27	0
3f	1	−98.66	−75.26	−23.40	0
3b	0	−98.44	−90.79	−7.66	0
3d	0	−96.70	−82.39	−14.31	0
3i	0	−93.07	−84.42	−8.65	0
3e	1	−89.18	−84.61	−4.58	0
3a	0	−88.90	−66.30	−22.60	0
3c	0	−88.78	−81.78	−7.00	0
3j	0	−88.49	−86.64	−1.85	0
3h	0	−88.09	−70.57	−17.52	0

According to the docking scores, compound **3g** showed the lowest total energy, which indicates it best fits into the active site of PDE5. The energy of the interactions between protein residue and ligand **3g** are tabulated in Table 5.

Table 5. The energy of the main interactions between protein PDE5 residue and ligand **3g.**

H Bond	Energy	Van Der Waals Interaction	Energy
S-Gln817	−6.81	S-Phe820	−18.51
S-His613	−3.41	S-Tyr612	−10.33
		S-Val782	−8.70
		S-Phe786	−7.90
		M-Leu765	−4.20
		S-Leu765	−4.04
		S-Met816	−4.01

(M = main chain; S = side chain).

Potential surface representation of PDE5 binding site with docked compound **3g** is presented in Figure 3, while Figure 4 illustrates the interactions of ligand **3g** with receptor PDE5 in the binding site.

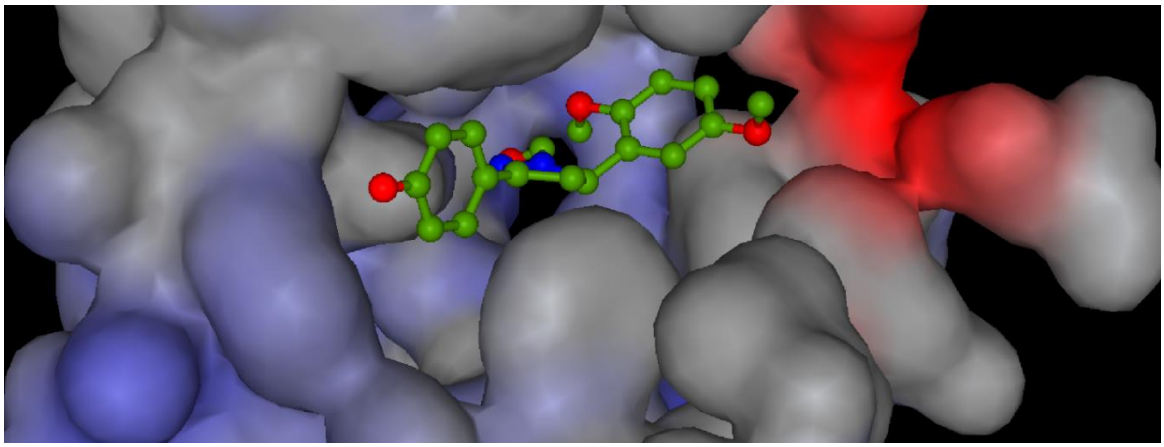

Figure 3. Potential surface representation catalytic domain of PDE5 with docked compound **3g**. (Range of potential: from min. 1.77 mV (blue) to max. 0.541 mV (red)).

The binding site of PDE5 was defined according to the inhibitor- -halogen derivate of monocyclic pyrimidinones (PDB ID: 5IO). Molecular docking confirmed the previous findings of characteristic binding interactions of inhibitors with the PDE5 catalytic domain [29]. Key interactions of compound **3g** are bidentate hydrogen bond (H-bond) with the side-chain of Gln817. One H-bond is formed with an oxygen atom of the carbaldehyde, and the second one with the nitrogen atom of pyrazole ring (Figure 4). Based on van der Waals interactions, pyrazole ring interacts with the side chain of Phe820. Side chain of Val782 forms π-π interactions with pyrazole ring and dimethoxyphenyl ring. The same ring is bonded to the Tyr612 by the π-donor hydrogen bond. Interactions of fluorophenyl ring are mediated through the π-σ interactions with Phe786 and π- sulfur interactions with Met816.

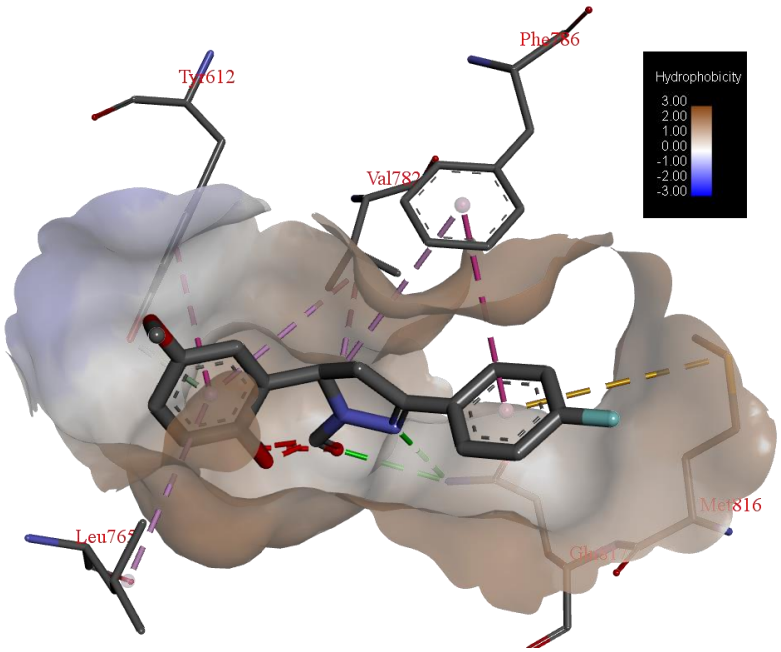

(**A**)

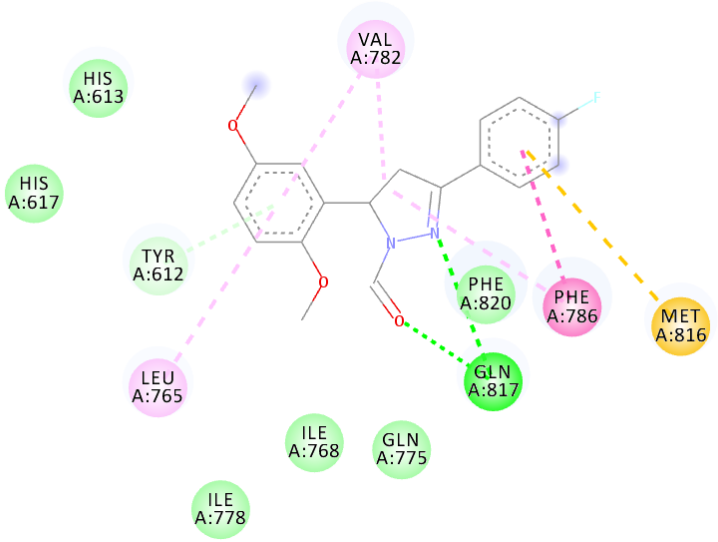

(**B**)

Figure 4. The main interactions of compound **3g** with residues in catalytic domain of PDE5: (**A**) 3D representation and hydrophobic surface of the binding site, (**B**) 2D representation (green = conventional hydrogen bond, light green = van der Waals, very light green = π-donor hydrogen bond, purple = π-σ interactions, light purple = π- πinteractions, pink = alkyl and π-alkyl interactions, brown = π-sulphur bond).

Docking results of this study are in accordance with the solved crystal structure of PDE5 catalytic domain in complex with different inhibitors. The catalytic domain of PDE5 includes three subdomains: N-terminal cyclin-fold region, a linker region and a C-terminal helical bundle in which the center is an active site of PDE5 core pocket (Q pocket) of the binding site contains Gln817, Phe820, Val782, Tyr612 [30]. Typical interactions include mono or bidentate hydrogen bonds of inhibitors with Gln817 and mainly π-π interactions of aromatic rings with hydrophobic clamp, which contains residuals, Val782, and Phe820. In the crystal structure of complex PDE5/sildenafil (PDB ID: 1UDT and 2H42) was confirmed the bidentate H-bonds are formed between the amide moiety of the pyrazolopyrimidinone of sildenafil and the side-chain of Gln817. Sildenafil (Viagra®) is a PDE5 inhibitor, which is approved as the first oral medicine for the treatments of male erectile dysfunction and for treatment of pulmonary arterial hypertension [29]. Previously mentioned ligand, 5IO [23], also formed classical bidentate H-bonds with residue Gln817, π-π interactions of phenyl ring with Phe820 and hydrophobic interactions with residues Leu765, Val782, Ala783, and Phe786. Moreover, halogen bonding interactions, between Tyr612 and I atom have been recognized.

4. Conclusions

In general, Gram-positive bacteria had higher resistance against tested compounds than Gram-negative bacteria. Fluorine, as the most electronegative element, modifies electron distribution which can diversify cell surface permeability leading to cell death. Since the experiment has proven that synthesized compounds are inactive as inhibitors of tyrosinase, a docking study has been performed and has indicated that the compound with the dimethoxyphenyl ring could be potent as an inhibitor of phosphodiesterase.

Author Contributions: Conceptualization, M.M.; methodology, H.B., M.M., V.R., I.S., M.L., M.K. and V.P.; software, V.R.; validation, M.M., V.P. and V.R.; formal analysis, V.R. and V.P.; investigation, H.B., I.S., M.L. and M.K.; resources, M.M.; data curation, M.M., V.P., and V.R.; writing—original draft preparation, V.P.; writing—review and editing, V.P., V.R.; visualization, M.M.; supervision, V.P.; project administration, V.R.; funding acquisition, V.P.

Funding: This research received no external funding.

Conflicts of Interest: The authors declare no conflict of interest.

References

1. Alam, J.; Alam, O.; Alam, P.; Naim, M.J. A Review on pyrazole chemical entity and biological activity. *Int. J. Pharm. Sci. Res.* **2015**, *6*, 1433–1442.
2. Alex, J.M.; Kumar, R. 4,5-Dihydro-1H-pyrazole: An indispensable scaffold. *J. Enzyme Inhib. Med. Chem.* **2014**, *29*, 427–442. [CrossRef] [PubMed]
3. Liu, P.; Hao, J.-W.; Mo, L.-P.; Zhang, Z.-H. Recent advances in the application of deep eutectic solvents as sustainable media as well as catalysts in organic reactions. *RSC Adv.* **2015**, *5*, 48675–48704. [CrossRef]
4. Shingare, R.M.; Patil, Y.S.; Gadekar, S.; Sangshetti, J.N.; Madje, B.R. Synthesis and antibacterial screening of novel 1,3,5-triaryl-4,5-dihydro-1H-pyrazole derivatives. *Morocc. J. Chem.* **2017**, *5*, 177–185.
5. Zhao, M.-Y.; Yin, Y.; Yu, X.-W.; Sangani, C.B.; Wang, S.-F.; Lu, A.-M.; Yang, L.-F.; Lv, P.-C.; Jiang, M.-G.; Zhu, H.-L. Synthesis, biological evaluation and 3D-QSAR study of novel 4,5-dihydro-1H-pyrazole thiazole derivatives as BRAFV600E inhibitors. *Bioorg. Med. Chem.* **2015**, *23*, 46–54. [PubMed]
6. Zhou, Z.; Zhuo, J.; Yan, S.; Ma, L. Design and synthesis of 3,5-diaryl-4,5-dihydro-1H-pyrazoles as new tyrosinase inhibitors. *Bioorg. Med. Chem.* **2013**, *21*, 2156–2162. [CrossRef] [PubMed]
7. Strunecká, A.; Patočka, J.; Connett, P. Fluorine in medicine. *J. Appl. Biomed.* **2004**, *2*, 141–150. [CrossRef]
8. Park, B.K.; Kitteringham, N.R.; O'Neill, P.M. Metabolism of fluorine-containing drugs. *Annu. Rev. Pharmacol. Toxicol.* **2001**, *41*, 443–470. [CrossRef]
9. Banday, A.H.; Mir, B.P.; Lone, I.H.; Suri, K.A.; Kumar, H.M.S. Studies on novel D-ring substituted steroidal pyrazolines as potential anticancer agents. *Steroids* **2010**, *75*, 805–809. [CrossRef] [PubMed]
10. Barsoum, F.F.; Girgis, A.S. Facile synthesis of bis(4,5-dihydro-1H-pyrazole-1-carboxamides) and their thio-analogues of potential PGE(2) inhibitory properties. *Eur. J. Med. Chem.* **2009**, *44*, 2172–2177. [CrossRef]

11. Bandgar, B.P.; Adsul, L.K.; Chavan, H.V.; Jalde, S.S.; Shringare, S.N.; Shaikh, R.; Meshram, R.J.; Gacche, R.N.; Masand, V. Synthesis, biological evaluation, and docking studies of 3-(substituted)-aryl-5-(9-methyl-3-carbazole)-1H-2-pyrazolines as potent anti-inflammatory and antioxidant agents. *Bioorg. Med. Chem. Lett.* **2012**, *22*, 5839–5844. [CrossRef] [PubMed]
12. Ozdemir, Z.; Kandilci, H.B.; Gümüşel, B.; Caliş, U.; Bilgin, A.A. Synthesis and studies on antidepressant and anticonvulsant activities of some 3-(2-furyl)-pyrazoline derivatives. *Eur. J. Med. Chem.* **2007**, *42*, 373–379. [CrossRef] [PubMed]
13. Sachchar, S.P.; Singh, A.K. Synthesis of some new fluorinated heteroaryl pyrazolines and isooxazolines as potential biocidal agents. *J. Indian Chem. Soc.* **1986**, *62*, 142–146. [CrossRef]
14. Camacho, M.E.; León, J.; Entrena, A.; Velasco, G.; Carrión, M.D.; Escames, G.; Vivó, A.; Acuña-Castroviejo, D.; Gallo, M.A.; Espinosa, A. 4,5-Dihydro-1H-pyrazole derivatives with inhibitory nNOS activity in rat brain: Synthesis and structure−Activity relationships. *J. Med. Chem.* **2004**, *47*, 5641–5650. [CrossRef] [PubMed]
15. Dabholkar, V.; Ansari, F. Synthesis and characterization of selected fused isoxazole and pyrazole derivatives and their antimicrobial activity. *J. Serb. Chem. Soc.* **2009**, *74*, 1219–1228. [CrossRef]
16. Gressler, V.; Moura, S.; Flores, A.F.C.; Flores, D.C.; Colepicolo, P.; Pinto, E. Antioxidant and antimicrobial properties of 2-(4,5-dihydro-1H-pyrazol-1-yl)-pyrimidine and 1-carboxamidino-1H-pyrazole derivatives. *J. Braz. Chem. Soc.* **2010**, *21*, 1477–1483. [CrossRef]
17. Liu, J.-J.; Sun, J.; Fang, Y.-B.; Yang, Y.-A.; Jiao, R.-H.; Zhu, H.-L. Synthesis, and antibacterial activity of novel 4,5-dihydro-1H-pyrazole derivatives as DNA gyrase inhibitors. *Org. Biomol. Chem.* **2014**, *12*, 998–1008. [CrossRef]
18. Rostom, S.A.F.; Badr, M.H.; Abd El Razik, H.A.; Ashour, H.M.A.; Abdel Wahab, A.E. Synthesis of some pyrazolines and pyrimidines derived from polymethoxy chalcones as anticancer and antimicrobial agents. *Arch. Pharm.* **2011**, *344*, 572–587. [CrossRef]
19. Molnar, M.; Kovač, T.; Strelec, I. Umbelliferone-thiazolidinedione hybrids as potent mushroom tyrosinase inhibitors. *Int. J. Pharm. Res. Allied Sci.* **2016**, *5*, 305–310.
20. Poroikov, V.V.; Filimonov, D.A.; Ihlenfeldt, W.-D.; Gloriozova, T.A.; Lagunin, A.A.; Borodina, Y.V.; Stepanchikova, A.V.; Nicklaus, M.C. PASS biological activity spectrum predictions in the enhanced open NCI database browser. *J. Chem. Inf. Comput. Sci.* **2003**, *43*, 228–236. [CrossRef]
21. Hocquet, A.; Langgård, M. An evaluation of the MM+ force field. *J. Mol. Med.* **1998**, *4*, 94–112. [CrossRef]
22. Stewart, J.J.P. Optimization of parameters for semiempirical methods V: Modification of NDDO approximations and application to 70 elements. *J. Mol. Model.* **2007**, *13*, 1173–1213. [CrossRef]
23. Ren, J.; He, Y.; Chen, W.; Chen, T.; Wang, G.; Wang, Z.; Xu, Z.; Luo, X.; Zhu, W.; Jiang, H.; et al. Thermodynamic and structural characterization of halogen bonding in protein–ligand interactions: A case study of PDE5 and its inhibitors. *J. Med. Chem.* **2014**, *57*, 3588–3593. [CrossRef] [PubMed]
24. Vollmer, W.; Blanot, D.; de Pedro, M.A. Peptidoglycan structure and architecture. *FEMS Microbiol. Rev.* **2008**, *32*, 149–167. [CrossRef] [PubMed]
25. Perkins, H.R. *Microbial Cell Walls and Membranes*; Springer: Dordrecht, The Netherlands, 1980; ISBN 978-94-011-6016-2.
26. Böhm, H.-J.; Banner, D.; Bendels, S.; Kansy, M.; Kuhn, B.; Müller, K.; Obst-Sander, U.; Stahl, M. Fluorine in medicinal chemistry. *ChemBioChem* **2004**, *5*, 637–643. [CrossRef] [PubMed]
27. Shah, P.; Westwell, A.D. The role of fluorine in medicinal chemistry. *J. Enzyme Inhib. Med. Chem.* **2007**, *22*, 527–540. [CrossRef]
28. Schellack, N.; Agoro, A. A review of phosphodiesterase type 5 inhibitors. *S. Afr. Fam. Pract.* **2014**, *56*, 96–101. [CrossRef]
29. Wang, X.-H.; Wang, X.-K.; Liang, Y.-J.; Shi, Z.; Zhang, J.-Y.; Chen, L.-M.; Fu, L.-W. A cell-based screen for anticancer activity of 13 pyrazolone derivatives. *Chin. J. Cancer* **2010**, *29*, 980–987. [CrossRef] [PubMed]
30. Sung, B.-J.; Hwang, K.Y.; Jeon, Y.H.; Lee, J.I.; Heo, Y.-S.; Kim, J.H.; Moon, J.; Yoon, J.M.; Hyun, Y.-L.; Kim, E.; et al. Structure of the catalytic domain of human phosphodiesterase 5 with bound drug molecules. *Nature* **2003**, *425*, 98–102. [CrossRef] [PubMed]